Short communication

A high-surface-area La-Ce-Mn mixed oxide with enhanced activity for CO and C$_3$H$_8$ oxidation

Baohuai Zhao[a], Rui Ran[a,*], Li Sun[a], Zesheng Yang[a], Xiaodong Wu[a], Duan Weng[a,b]

[a] State Key Laboratory of New Ceramic and Fine Processing, School of Materials Science and Engineering, Tsinghua University, Beijing 100084, China
[b] Key Laboratory of Advanced Materials (MOE), School of Materials Science and Engineering, Tsinghua University, Beijing 100084, China

ARTICLE INFO

ABSTRACT

A high-surface-area La-Ce-Mn mixed oxide was synthesized by citrate method, with further acid etching to dissolve the La^{3+} ions in the lattice. The acid etching process efficiently improved the specific surface area, increased the ratios of Mn^{4+}/Mn^{n+}, Ce^{3+}/Ce^{n+}, O$_\alpha$/O$_{tot}$, and enhanced the oxygen mobility of the catalyst, which were responsible for the superior catalytic performance. Compared to the pristine La$_{0.8}$Ce$_{0.2}$MnO$_{3+\delta}$ catalyst, the etched one could convert CO and C$_3$H$_8$ more efficiently, with 90% conversion of CO and C$_3$H$_8$ at only 73 and 196 °C, respectively. Such superior catalytic performance made it possible to be used for automotive emission control during cold-start period.

1. Introduction

The rise of more strict environmental regulations has set new challenges for the development of automotive catalysts around the world. It was reported that 50–80% of the CO and total hydrocarbons (HCs) were produced from automobiles during the cold-start period [1–5]. Conventional automotive catalysts are generally not efficient enough to remove these pollutants due to the lower temperature (< 200 °C) of emissions. Thus, developing more effective low-temperature catalysts especially with low cost is of much importance.

Owing to its considerable oxidative catalytic activity and lower price compared to precious metal catalysts [6–8], the LaMnO$_{3+\delta}$ perovskite-type oxide would be a promising material for the emission control during the cold-start period. Its activity can be further improved by replacing La with other ions that have different radii or valence states [6,9]. Among the diverse substitutions, Ce had remarkable effects to promote the oxidation of CO and C$_3$H$_8$, and the optimized ratio of La/Ce/Mn was 0.8/0.2/1 [10,11]. However, the perovskite particles are easily agglomerated after sintering and hold a low specific surface area (< 10 m^2 g^{-1}) [10,12]; and their catalytic activities at low temperatures cannot meet the requirements for eliminating pollutants during the cold-start period.

Acid etching of the LaMnO$_{3+\delta}$ perovskite was an effective method to improve both specific surface area and catalytic oxidation activity [12–15]. During the etching process, La was selectively removed from the perovskite structure to produce more defects in the oxide, accompanied by the formation of MnO$_x$, such as γ-MnO$_2$ phase or amorphous

manganese oxides [13–15]. As Ce is not easy to be removed by acid etching and would act as a catalytic promoter, it is worthy to investigate the effects of the acid etching on the La$_{0.8}$Ce$_{0.2}$MnO$_{3+\delta}$ catalyst.

In this work, the Ce-doped LaMnO$_{3+\delta}$ perovskite was treated by the acid etching method to prepare a La-Ce-Mn mixed oxide catalyst. The differences of physical and chemical properties between the pristine catalyst and the etched one were investigated by various characterizations, in order to verify the potential of such a material as a low-temperature oxidation catalyst for automotive emission control during cold-start period.

2. Experimental

2.1. Catalyst synthesis

A citrate method, which was similar to the procedure in literature [12], was adopted to synthesize La$_{0.8}$Ce$_{0.2}$MnO$_{3+\delta}$, using La(NO$_3$)$_3$·6H$_2$O (99.9%, Aladdin, China), Ce(NO$_3$)$_2$·6H$_2$O (99.5%, Aladdin, China), Mn(NO$_3$)$_2$ (aqueous solution, 50 wt%, Aladdin, China), and citric acid (99.5%, Aladdin, China). The nitrates with a stoichiometric ratio were dissolved in deionized water. Then 10% excess citric acid over the total number of ionic equivalents of cations was added to the aqueous solution to guarantee a complete complexation of the metal ions. The resulting solution was evaporated at 90 °C under vigorous stirring to get a gel. Then a spongy amorphous citrate precursor was obtained after the gel was dried at 110 °C in an oven

---

overnight. The citrate precursor was milled and calcined in static air at 300 °C for 1 h to decompose the organics, then heated to 750 °C and held for 5 h. The heating rate was 1 °C min^{-1} in the calcination process.

In the following acid etching process, the as-obtained $La_{0.8}Ce_{0.2}MnO_{3+\delta}$ was put into the HNO_3 solution (1 mol L^{-1}) and stirred for 24 h. The product was washed with deionized water until the filtrated water was neutral. After being dried at 110 °C overnight, a calcination process at 300 °C for 3 h in static air with a heating rate of 10 °C min^{-1} was used to obtain the catalyst. For a good comparison, the pristine $La_{0.8}Ce_{0.2}MnO_{3+\delta}$ sample was also washed, dried, and calcined in the same procedure. The final samples were denoted as LCMO and LCMO-24 for the original material and the etched one, respectively.

2.2. Characterizations

2.2.1. Material characterization

X-ray diffraction (XRD) was carried out to detect the phase structures of the catalysts. The morphologies were observed using scanning electron microscopy (SEM) and transmission electron microscopy (TEM). The pore volumes and specific surface areas were determined by N_2 adsorption/desorption experiments. The X-ray photoelectron spectroscopy (XPS) experiments were performed to get the surface properties. O_2 temperature-programmed desorption (O_2-TPD) and H_2 temperature-programmed reduction (H_2-TPR) were performed to evaluate the redox properties of the catalysts. All of the characterizations mentioned above can be found in detail in our previous work [12,16,17].

2.2.2. Activity measurement

The catalytic oxidation of CO and C_3H_8 were performed in a fixed-bed quartz reactor (i.d. 5 mm) filled with 100 mg catalyst. Prior to the test, the catalyst was pretreated in 10% O_2/N_2 at 300 °C for 30 min. Then the temperature was cooled down to 0 °C rapidly and the reactant gas mixture (5000 ppm CO or C_3H_8, 10% O_2 balanced with N_2) was introduced into the reactor. The flow rate was 100 ml min^{-1}, corresponding to a gas hourly space velocity (GHSV) of 60,000 ml g$_{cat}^{-1}$ h^{-1}. After the gas concentration was stable for 10 min, the temperature was increased from 0 to 300 °C and 350 °C for CO and C_3H_8 oxidation, respectively. The temperature heating rate was 10 °C min^{-1}. The outlet gas was analyzed using an FTIR gas analyzer (MKS Multigas™ 2030 gas-phase). The CO conversion and C_3H_8 conversion were calculated as:

$$CO_{conv.} (\%) = (1 - [CO]_{outlet}/[CO]_{inlet}) \times 100\% \qquad (1)$$

$$C_3H_{8conv.} (\%) = (1 - [C_3H_8]_{outlet}/[C_3H_8]_{inlet}) \times 100\% \qquad (2)$$

The activity tests were performed twice and the second run was chosen to evaluate the catalytic activity.

3. Results and discussion

3.1. Phase structures and morphologies

Fig. 1 shows the diffraction patterns of the samples. The intense diffraction peaks marked with stars are correlated with those of the rhombohedral $LaMnO_{3.26}$ (JCPDS #50-0299) [8,9]. The perovskite diffraction peaks of the etched sample LCMO-24 have lower intensities, indicating its poorer crystallinity compared to LCMO. The diffraction peaks at 28.6 and 56.4° indicate the presence of cubic CeO_2 (JCPDS #81-0792) in the two catalysts, which is in agreement with the results in the literature [9,11,18,19] that not all of the Ce atoms were incorporated into the perovskite lattice with such an atomic ratio. A weak diffraction peak at 37.1° that exists only in the pattern of LCMO-24 shows the formation of manganese oxide after etching. The LCMO-24 sample should be therefore an oxide mixture containing CeO_2, MnO_x, and perovskite.
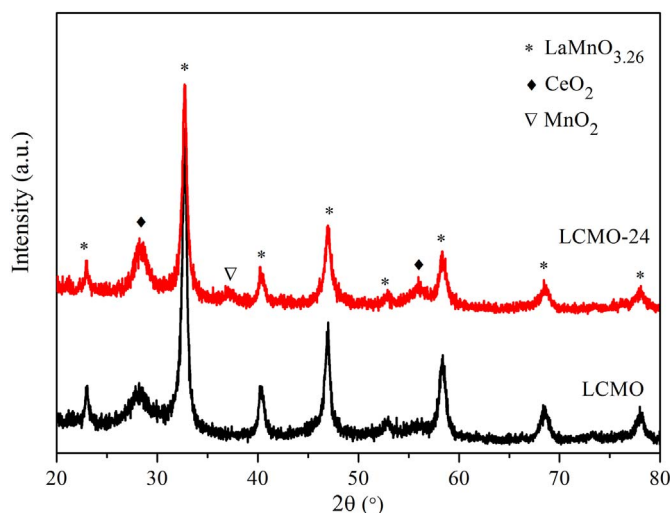

Fig. 1. XRD patterns of LCMO and LCMO-24.

Fig. 2 shows the microscopic analysis images of the two catalysts. In the SEM images, LCMO displays many severely sintered particles which are tightly contacted with their adjacent ones, while LCMO-24 presents a porous structure. Element compositions realized by EDS are shown in Table 1. Less La is found in LCMO-24 than in LCMO but Ce remains after acid etching, suggesting the successful selectively removing of La atoms by acid etching. TEM images of the two catalysts show the amplifying morphologies of LCMO and LCMO-24, respectively, which confirm the severely sintered status of LCMO and the porous structure of LCMO-24. The SAED patterns of the two catalysts are shown as insets in the HR-TEM images. The multiple bright electron diffraction rings demonstrate that both samples are polycrystalline. The fringe distances of 3.85 Å, 2.74 Å, and 2.24 Å represent the lattice spacings of the (012), (110), and (202) planes of $LaMnO_{3.26}$, respectively. The fringe distances of 3.12 Å and 2.71 Å are assigned to the lattice spacings of the (111) and (200) planes of CeO_2, respectively. Both $LaMnO_{3.26}$ and CeO_2 phases are found in each of the catalysts, which is in line with the XRD results. The specific surface area of LCMO and LCMO-24 are 26.1 and 111.5 m^2 g^{-1}, respectively. The pore volume of LCMO-24 is 0.43 cm^3 g^{-1}, which is over three times that of LCMO (0.13 cm^3 g^{-1}). It confirms that the acid etching can extensively improve the specific surface area and pore volume of the catalyst.

3.2. Surface properties

The surface atomic content of La, Ce, Mn, and O determined by XPS is shown in Table 1. It is seen that the La content decreases after the acid etching process while Ce still remains in the catalyst, which is in agreement with the EDS results. All the XPS spectra (Fig. S1) of Mn 2p, Ce 3d, and O1s, as well as the information of peak assignments, are provided in the supplementary material. The atomic ratios calculated from the relative area of sub-peaks are summarized in Table 2. The Mn^{4+}/Mn^{n+} and Ce^{3+}/Ce^{n+} ratios are increased after the acid etching process. The O_α/O_{tot} ratio of LCMO-24 (31.1%) is also considerably higher than that of LCMO (25.1%), indicating the formation of surface-labile oxygen species after acid etching [8,13,20]. For the oxygen species in the catalysts, the surface oxygen species (O_α) is widely accepted to be more reactive for oxidation reactions than the lattice oxygen species (O_β) because of its higher mobility [21].

3.3. Reducibility

The reducibilities of the catalysts were detected by H_2-TPR experiments and the results are shown in Fig. 3. Four reduction peaks marked as α, β, γ, and δ are found in each of the curves. Peak α is due to the